Topological protection of Majorana polaritons in a cavity

Zeno Bacciconi [1,2] Gian Marcello Andolina,[3] and Christophe Mora[4]
[1]*International School of Advanced Studies (SISSA), via Bonomea 265, 34136 Trieste, Italy*
[2]*The Abdus Salam International Centre for Theoretical Physics (ICTP), Strada Costiera 11, 34151 Trieste, Italy*
[3]*JEIP, USR 3573 CNRS, Collège de France, PSL Research University, 11 Place Marcelin Berthelot, F-75321 Paris, France*
[4]*Université Paris Cité, CNRS, Laboratoire Matériaux et Phénomènes Quantiques, 75013 Paris, France*

(Received 9 October 2023; revised 16 February 2024; accepted 12 March 2024; published 22 April 2024)

Cavity embedding is an emerging paradigm for the control of quantum matter, offering avenues to manipulate electronic states and potentially drive topological phase transitions. In this work, we address the stability of a one-dimensional topological superconducting phase to the vacuum quantum fluctuations brought by a global cavity mode. By employing a quasiadiabatic analytical approach completed by density matrix renormalization group calculations, we show that the Majorana end modes evolve into composite polaritonic modes while maintaining the topological order intact and robust to disorder. These Majorana polaritons keep their non-Abelian exchange properties and protect a twofold exponentially degenerate ground state for an open chain. They become, however, weak edge modes in the sense that they no longer commute with the full Hamiltonian and protect the exponential degeneracy only in the ground-state manifold.

DOI: 10.1103/PhysRevB.109.165434

I. INTRODUCTION

In recent years the possibility of controlling quantum matter by cavity embedding has attracted a lot of attention [1–4]. Strong coupling to cavity vacuum fluctuations has been predicted to affect material properties in many different contexts such as superconductivity [5–7], ferroelectricity [8–10], and topology [11–15]. It has been shown experimentally that cavity embedding can modify the critical temperature of a charge density wave transition [16], magnetotransport properties [17], and induce the breakdown of topological protection in integer quantum Hall transport [18]. In this context, a single-particle electron-photon Chern number was introduced in Ref. [19]. Addressing topological properties with a global cavity mode is a subtle issue. As a general rule, the robustness of topological properties is ensured by the locality of perturbations. Coupling to a cavity is inherently nonlocal, and therefore there is no guarantee that quantum fluctuations preserve topological protection. A contrasting argument in the context of Majorana fermions is that they bear no charge and therefore couple inefficiently to a cavity electric field [20] (see also Refs. [21–25] in the context of microwave resonators). Naive expectations relying on the weak effect of vacuum fluctuations of single-mode cavities on extensive quantities [26–28] should also be taken with care since topological edge states are intrinsically not extensive.

In this work, we address this issue by studying a one-dimensional (1D) toy model of a topological superconductor [29,30], featuring Majorana end states, strongly coupled to a single-mode cavity, and therefore interacting [31–34] via long-range forces. We discuss two models for the cavity, either with an electric field [17,18] or a magnetic field coupling [35–37]. Both models respect the fermionic parity $\mathbb{Z}_2$ symmetry of the superconductor [29]. Our approach to studying these many-body topological properties is twofold. We first employ analytical arguments, based on quasiadiabatic continuation approach [38,39], to establish the resilience of the topological phase to the all-to-all interaction mediated by the cavity mode. The edge modes transform into Majorana polaritons [21] with a light component and are no longer purely fermionic objects. We also perform controlled density matrix renormalization group (DMRG) numerical simulations [40–42] with a mixed cavity-matter matrix product state (MPS) ansatz [14,43–45] implementing the $\mathbb{Z}_2$ fermionic parity. We identify four markers for topological order [39,46,47]: (i) ground-state degeneracy, (ii) entanglement spectrum degeneracy, (iii) nonlocal edge-edge correlations, and (iv) robustness to local symmetry-preserving perturbations (e.g., disorder), and demonstrate that they all survive strong cavity quantum fluctuations. We moreover confirm the hybrid nature of the dressed Majorana end operators. Our main finding is that the topological superconducting state is robust to the coupling to the cavity, by adapting its Majorana edge modes, as long as fermionic parity is preserved and no gap closing occurs upon gradually increasing the strength of cavity coupling. Additionally, Majorana in the absence of a cavity are strong edge modes [48], which commute with the Hamiltonian, imposing an exponential degeneracy in the full spectrum. In contrast, we find that they change into weak edge modes [38,49,50] and lose commutation with the Hamiltonian as they combine with light into composite polaritons. This restricts the exponential degeneracy to the ground-state manifold.

The paper is structured as follows. In Sec. II, we introduce the toy model illustrating a topological superconductor and its coupling to the nonlocal cavity degree of freedom. Section III presents a comprehensive numerical analysis covering all relevant topological properties (i)–(iv). Following this, Sec. IV applies the quasiadiabatic continuation approach, crucial for understanding the resilience of Majorana fermions to nonlocal cavity fluctuations. In Sec. V, perturbative analytical expressions are derived highlighting the composite character of the Majorana polaritons. They are shown to be weak edge modes, localized for their fermionic part on the edges of the chain. Finally, in Sec. VI we draw general conclusions about the stability of Majorana fermions to nonlocal cavity fluctuations and discuss possible extensions of our arguments to other topological states of matter.

II. MODEL

The starting point of our discussion is a tight-binding model for a one-dimensional topological superconductor. We employ a toy model of spinless electrons hopping on a square ladder geometry [45] in the presence of an external magnetic field and a superconducting pairing along the rung of the ladder. The Hamiltonian reads:

$$\hat{H}_0 = -t\sum_{j=1}^{L-1} e^{i\sigma\phi_{\text{ext}}/2}\hat{c}^\dagger_{\sigma,j}\hat{c}_{\sigma,j+1} - t_\perp\sum_{j=1}^{L}\hat{c}^\dagger_{+,j}\hat{c}_{-,j} + \Delta\sum_{j=1}^{L}\hat{c}^\dagger_{+,j}\hat{c}^\dagger_{-,j} + \mu\sum_{\sigma,j=1}^{L}\hat{c}^\dagger_{j,\sigma}\hat{c}_{j,\sigma} + \text{H.c.}, \tag{1}$$

where Δ is the pairing strength, μ the chemical potential, t the intraleg hopping, $t_\perp$ the interleg hopping, ϕ_{ext} the external magnetic flux per plaquette and $\hat{c}_{j,\sigma}$ annihilates an electron on the leg $\sigma = \pm$ and rung $j = 1,\dots,L$ with $+$ is the top leg and L the number of rungs. While unconventional, this model can be straightforwardly mapped to the nanowire model [51,52] with strong Rashba spin-orbit coupling and proximity-induced superconductivity, a system that has undergone extensive experimental investigation [53]. In the tenfold noninteracting classification [54], the model Eq. (1) falls into class D, protected only by particle-hole symmetry. It has a $\mathbb{Z}_2$ topological invariant and allows for a topological phase with Majorana end states. However, within a many-body context, the true symmetry protecting the topological phase is fermionic parity.

We now add a single-mode cavity with the bare Hamiltonian $\hat{H}_c = \hbar\omega_c\hat{a}^\dagger\hat{a}$. In order to draw general conclusions, we examine two distinct physical realizations concerning the vector potential in the cavity: a constant magnetic (B) component along z or a constant electric (E) component along y (Fig. 1). The light-matter coupling is achieved through a Peierls substitution [55–58], where the hoppings are dressed as:[1]

$$\text{B}: \hat{c}^\dagger_{\sigma,j}\hat{c}_{\sigma,j+1} \rightarrow e^{ig_B(\hat{a}+\hat{a}^\dagger)}\hat{c}^\dagger_{\sigma,j}\hat{c}_{\sigma,j+1}, \tag{2}$$

$$\text{E}: \hat{c}^\dagger_{+,j}\hat{c}_{-,j} \rightarrow e^{ig_E(\hat{a}+\hat{a}^\dagger)}\hat{c}^\dagger_{+,j}\hat{c}_{-,j}, \tag{3}$$

depending on the scenario. In the following discussion, when referring to both couplings, we will use g as a combined notation for g_E and g_B. The full Hamiltonian is $\hat{H} = \hat{H}_0 + \hat{H}_c$ with either the dressing of Eq. (2) or Eq. (3). We are interested in a mesoscopic regime and do not scale g with the system size. Our choice is motivated by the nature of strongly confined cavity modes in nanophotonics, such as split-ring resonators,

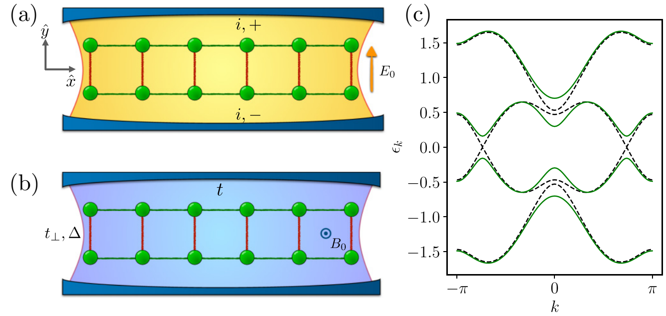

FIG. 1. Sketch of the two different cavity embeddings. The ladder couples either (a) to a quantized electric field, or (b) to a quantized magnetic field. (c) Band structure of the cavity-free Hamiltonian $\hat{H}_0$ with (full green line) and without (dashed black line) superconducting pairing.

where there are usually a few, energetically well-separated modes with a significant coupling to the electrons [18].

No-go theorems [26,60] prevent photon condensation, i.e., a coherent nonzero $\langle\hat{a}\rangle$, for the electric field coupling, whereas $\langle\hat{a}\rangle \neq 0$ can emerge in the magnetic case [61–63]. In the latter case, the coherent part of the field simply renormalizes ϕ_{ext} and can potentially drive the system out of a topological state or vice versa. Although very interesting, this effect does not come from quantum fluctuations and can be described semiclassically [45]. We henceforth fix $\omega_c = t = t_\perp = -\mu = 1$, $\Delta = 0.4$ and $\phi_{\text{ext}} = 0.6889\pi$ such that $\langle\hat{a}\rangle$ remains close to zero and the fermionic chain is in a topological phase.

III. SIGNATURES OF TOPOLOGY

We first present a detailed DMRG numerical investigation of the topological properties of the ground state of the Hamiltonian $\hat{H}$. We use a hybrid light-matter MPS in which the $\mathbb{Z}_2$ fermionic parity symmetry is implemented [59], separating the exponentially degenerate even and odd parity sectors. We specifically investigate the four markers, labeled (i)–(iv) in the introduction, as signatures of the topological phase.

The ground-state degeneracy $\Delta E_{gs} = |E^{gs}_0 - E^{gs}_1|$ is exponential with the system size up to relatively strong light-matter couplings g, confirming point (i). This is reported in Figs. 2(a), 2(d) where the ground-state energy difference between the two parity sectors is computed. For small g, this energy difference can also be evaluated using perturbation theory [59], confirming its exponential scaling. Interestingly we also report of few ground-state parity switches [29,64] as a function of g (not shown). The second signature (ii) is the twofold degeneracy in the entanglement spectrum of the half-chain bipartition. Differing from typical fermionic Hamiltonians, the coupling to the cavity introduces nonlocality and a choice for where to park the cavity in a bipartition of the system. We use an alternative way of partitioning by tracing out the cavity field,

$$\hat{\rho}_{j>L/2} = \text{Tr}_{j<L/2}[\hat{\rho}_{\text{matt}}] = \text{Tr}_{j<L/2}[\text{Tr}_{ph}[|gs\rangle\langle gs|]], \tag{4}$$

where $|gs\rangle$ is the full many-body ground state, $\hat{\rho}_{\text{matt}}$ the reduced density matrix after tracing out the photons. $\hat{\rho}_{j>L/2}$ is obtained by further tracing out half of the chain. As shown in

[1] See Supplemental Material [59].

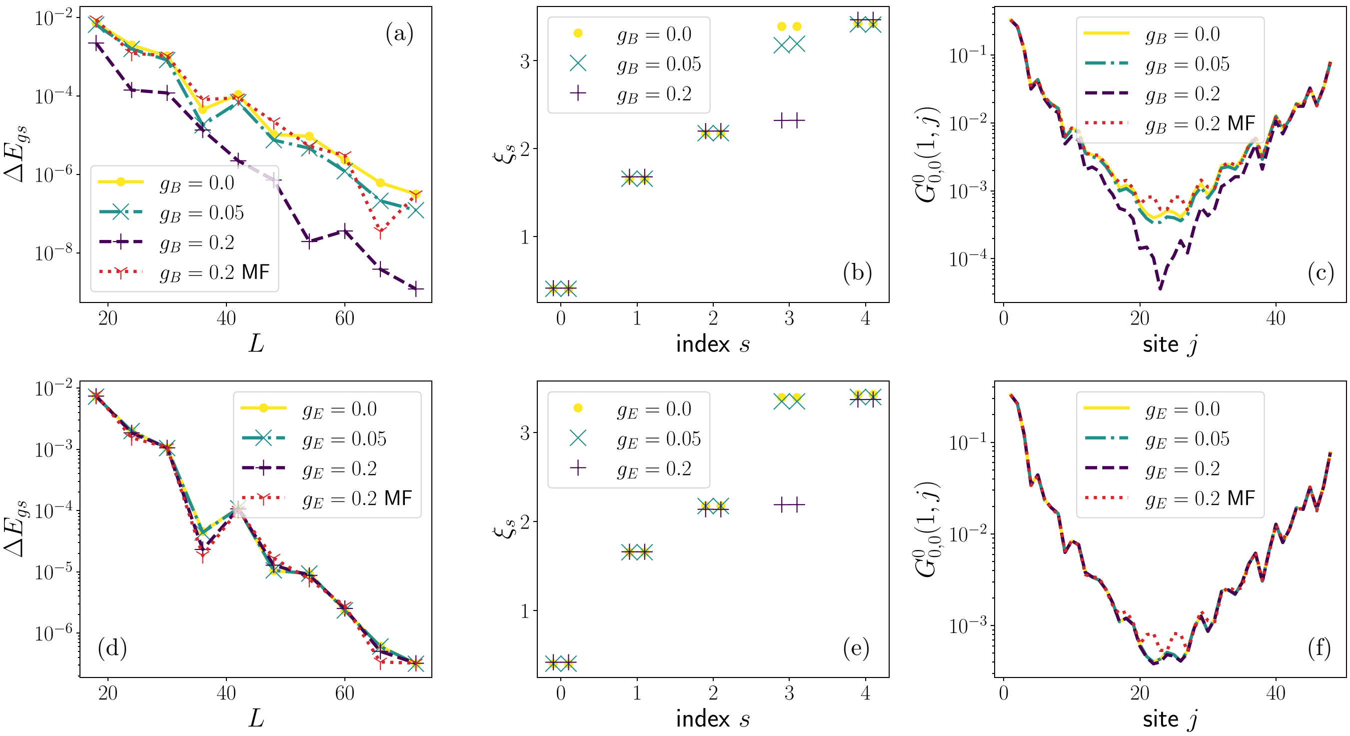

FIG. 2. The top (bottom) row shows DMRG results for the magnetic (electric) coupling. (a), (d) Ground-state energy splitting $\Delta E_{gs} = |E_0^{gs} - E_1^{gs}|$ for different coupling strength. The mean-field (MF) result is also shown for comparison. (b), (e) Entanglement spectra $\xi_s = -\log\lambda_s$ for a half-chain bipartition of the ground state in the even parity sector. The twofold degeneracies come from (even, even) and (odd, odd) parity resolved partitions. (c), (f) Correlation function for the top leg of the ladder geometry. $L = 48$ except for (a), (e).

Figs. 2(b), 2(e) the $g = 0$ twofold degeneracy is not broken at finite g. It can be checked to correspond to the two choices of parity for each half. The entanglement spectra are nonetheless changing with g, signaling the presence of finite light-matter entanglement.

Edge-edge correlations (iii) are shown in Figs. 2(c), 2(f) where the correlator $G^p_{\sigma,\sigma'}(i, j) = \langle p|\,\hat{c}^\dagger_{\sigma,i}\hat{c}_{\sigma',j}\,|p\rangle$ is calculated on the ground state $|p\rangle$ with parity $p = \{0, 1\}$. The revival on the opposite edge of the Green's function reveals the presence of the two ends Majorana fermions that both permute the ground states and is essential to verify the nonlocal nature of the zero-energy mode. We now verify (iv) by adding local disorder to the model. Without loss of generality, we consider a Gaussian distributed chemical potential, centered around μ, and with the standard deviation $\overline{\delta\mu_{\sigma,i}\delta\mu_{\sigma',j}} = W^2\delta_{i,j}\delta_{\sigma,\sigma'}$, where $\overline{\mathcal{A}}$ denotes the disorder average of $\mathcal{A}$. As an indicator for edge-edge correlations, we introduce the quantity

$$Q = \sum_{\sigma,\sigma'} \left|G^0_{\sigma,\sigma'}(1, L) - G^1_{\sigma,\sigma'}(1, L)\right|. \tag{5}$$

For $g = 0$, we have exactly $G^0_{\sigma,\sigma'}(1, L) = -G^1_{\sigma,\sigma'}(1, L)$ as a result of the anticommutation of the two Majorana fermions. In Fig. 3, we show the indicator Q and the ground-state energy splitting ΔE_{gs} for one disorder realization at each disorder strength [Figs. 3(a), 3(c)] and their disorder average [Figs. 3(b), 3(d)]. The results hardly depend on the strength of cavity coupling, reflecting the robust topological phase. Interestingly, Kohn's theorem yields a different behavior in the quantum Hall effect, where disorder and cavity collaborate to diminish topological protection [11,15,65]. Here,

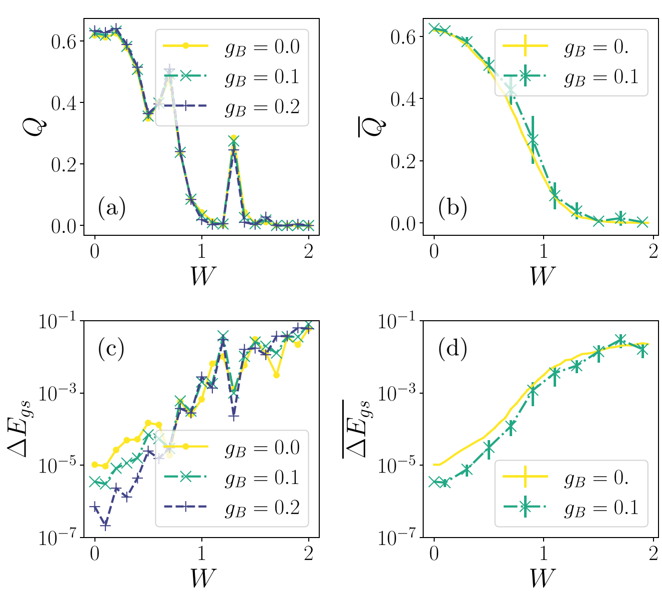

FIG. 3. Magnetic cavity: DMRG results ($g_B > 0$) and exact results ($g_B = 0$) for topological markers as a function of disorder strength W. (a) Edge-edge correlator Q from Eq. (5) and (c) ground-state degeneracy ΔE_{gs} for a single disorder realization at each strength W. The corresponding disorder averaged quantities are shown in (b), (d) with $N_{\rm dis} = 20\,(1000)$ realizations for $g_B = 0.1\,(0.)$. Error bars indicate two standard deviations and $L = 48$.

disorder plays no role in enhancing the cavity effect on Majorana fermions.

IV. QUASIADIABATIC CONTINUATION

In this section we present analytical arguments that elucidate the resilience of topological order to nonlocal cavity quantum fluctuations. In the absence of a cavity, the model exhibits Majorana edge modes in its topological phase. The Majorana fermionic operators $\hat{\gamma}_L^0$ and $\hat{\gamma}_R^0$ permute the even and odd parity sectors and protect the ground-state (exponential) degeneracy. We employ the theory of quasiadiabatic continuation [38,39] to show that the Majorana operators

$$\hat{\gamma}_L = \mathcal{V}\hat{\gamma}_L^0\mathcal{V}^\dagger \quad \hat{\gamma}_R = \mathcal{V}\hat{\gamma}_R^0\mathcal{V}^\dagger\,, \tag{6}$$

undergo a continuous transformation as the coupling to the cavity is gradually enhanced. The unitary operator $\mathcal{V}$ maps the ground-state manifold in the absence of a cavity to the one with the cavity. Importantly, under the assumption that the gradual increase of the cavity coupling maintains both the $\mathbb{Z}_2$ symmetry and a finite spectral gap, it can be shown [59] that $\mathcal{V}$ preserves fermionic locality such that the two deformed Majorana modes remain localized on the two ends of the chain. In addition, $\hat{\gamma}_L$ and $\hat{\gamma}_R$ acquire a finite entanglement with the cavity mode $\hat{a}$ from Eq. (6) and a polaritonic character associated with photonic excitations. They also keep satisfying the Clifford algebra, as $\mathcal{V}$ is unitary, and they permute the even- and odd-parity ground states.

Aside from the deformed edge Majorana modes, we also need to prove the persistence of the ground-state degeneracy. Denoting P_0 ($P = \mathcal{V}P_0\mathcal{V}^\dagger$) the projector onto the ground-state manifold without (with) cavity, it is known that [29,38]

$$P_0\mathcal{O}P_0 = \lambda\, P_0, \tag{7}$$

up to exponential corrections with the system size. Here, $\mathcal{O}$ is a local $\mathbb{Z}_2$-symmetric operator and λ its eigenvalue in the ground state. Physically, Eq. (7) simply states that a local perturbation cannot distinguish the two ground states because of topological order. Applying Eq. (7) for $\mathcal{O} = \hat{H}_0$ recovers the ground-state twofold degeneracy. $\mathcal{V}^\dagger\hat{H}\mathcal{V}$ is also local for fermions as $\mathcal{V}$ maintains locality. Therefore, we obtain that the even and odd parity states are still exponentially degenerate in the presence of the cavity, or

$$P\hat{H}P = \mathcal{V}P_0\mathcal{V}^\dagger\hat{H}\mathcal{V}P_0\mathcal{V}^\dagger = E_{gs}\mathcal{V}P_0\mathcal{V}^\dagger = E_{gs}P, \tag{8}$$

where E_{gs} is the energy of the two ground states. Furthermore, with no cavity, $[\hat{\gamma}_\alpha^0, \hat{H}_0] = 0$ (up to exponential corrections), which implies that the twofold degeneracy extends to the whole spectrum and the Majorana operators are called strong edge modes [39,48,49]. Such a vanishing commutator is no longer guaranteed in the presence of the cavity, that is $[\hat{\gamma}_\alpha, \hat{H}] \neq 0$. The deformed $\hat{\gamma}_\alpha$ are then weak edge modes as they do not enforce a twofold degeneracy for excited states, only in the ground-state manifold. We further elaborate on this point in the next section.

In Fig. 4 we numerically test the absence of gap closing and the evidence of transition from strong to weak edge modes as the coupling to the cavity is increased. Note that the degeneracy is lifted for a state whose energy ($\epsilon_k \simeq 0.33$) is much detuned from the cavity frequency ($\omega_c = 1$). The fact that different type of couplings produce different splittings is expected on the basis of the difference in interaction matrix elements. The weakening of the edge modes could be related to the predicted [25] sensitivity of the cavity damping to the parity of excited electronic states. Moreover, the comparison with a mean-field approach [59] (red lines) highlights the need for light-matter entanglement to quantitatively address strong coupling and the many-body nature of the spectrum.

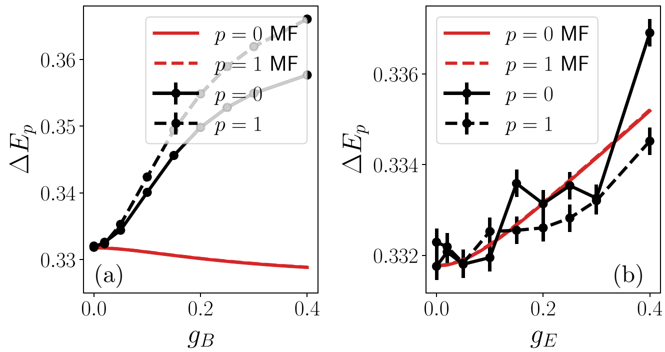

FIG. 4. Energy gap to the first excited state in the two parity sectors $p = 0$ (full lines) and $p = 1$ (dashed lines) calculated via DMRG. The red lines represent the mean-field predicted values of gaps. (a) and (b) show respectively the result for the magnetic coupling and electric coupling. $L = 48$.

Remarkably, the above arguments based on the quasiadiabatic continuation are very general. They show that any topological superconductor with Majorana end modes is robust to the presence of a nonlocal cavity, as long the coupling conserves parity ($\mathbb{Z}_2$) and there is an adiabatic path without gap closing to a cavity-free limit.

V. MAJORANA POLARITONS

In this section we discuss in more detail the composite light-matter nature of the edge modes. An explicit polaritonic form can be given to the Majorana fermions from Eq. (6) in perturbation theory

$$\hat{\gamma}_\alpha \simeq \hat{\gamma}_\alpha^0 + \sum_{n=(\sigma,j)} \left(\Psi_\alpha^{1+}(n)\hat{c}_n^\dagger\hat{a}^\dagger + \Psi_\alpha^{1-}(n)\hat{c}_n\hat{a}^\dagger + \text{H.c.}\right), \tag{9}$$

assuming weak coupling to the cavity. The wave function

$$\Psi_\alpha^{1+} = \psi_\alpha^{1+} + \phi_\alpha^{1+} = 2\sum_{\mu\neq 1}\frac{\lambda_\mu^\alpha u_{n,\mu}}{\epsilon_\mu + \omega_c} + 2\sum_{\mu\neq 1}\frac{\lambda_\mu^\alpha v_{n,\mu}^*}{\epsilon_\mu - \omega_c} \tag{10}$$

is obtained together with a similar expression for $\Psi_\alpha^{1-}(n)$ given in the Supplemental Material [59]. The coefficients λ_μ^α denote the projections of the perturbative cavity coupling onto the Bogoliubov modes diagonalizing Eq. (1) with energies ϵ_μ. $u_{n,\mu}$ and $v_{n,\mu}$ are the corresponding electron and hole components. The first term ψ_α^{1+} in Eq. (10) combines a photon creation with a Bogoliubov excitation whereas the second term (ϕ_α^{1+}) annihilates a Bogoliubov mode while still adding a photon. The second term ϕ_α^{1+} in Eq. (10) exhibits a divergence whenever the photon energy $\hbar\omega_c$ lies within the Bogoliubov spectrum and $\epsilon_{\mu_0} = \hbar\omega_c$ for a certain μ_0. As detailed in the Supplemental Material [59], this divergence can be cured by excluding the mode μ_0 (along with

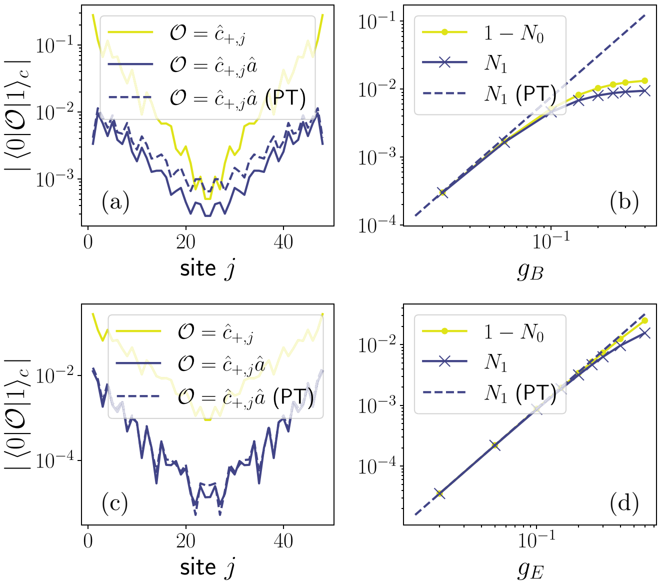

FIG. 5. (a), (c) Connected matrix elements revealing the hybrid nature of Majorana polaritons for (a) magnetic coupling $g_B = 0.1$ and (c) electric coupling $g_E = 0.4$, with zero ($\mathcal{O} = \hat{c}_{+,j}$) and one photon ($\mathcal{O} = \hat{c}_{+,j}\hat{a}$). (b), (d) Evolution of the total zero- and one-photon weights N_0 and N_1, Eq. (12), with light-matter coupling for the magnetic (b) and electric (d) cavities. Here $L = 48$.

modes with nearby energies) from the sum in Eq. (10) all the while preserving the properties of the quasiadiabatic continuation detailed in Sec. IV. However, the Majorana polaritons then fail to commute with the Hamiltonian, $[\hat{\gamma}\alpha, \hat{H}] \neq 0$, and consequently transition into weak edge modes. Since ϕ_α^{1+} annihilates Bogoliubov modes, the commutation with the Hamiltonian persists within the ground state, explaining its robust twofold degeneracy. A perturbation analysis to higher orders reveals additional divergences occurring when $n\hbar\omega_c = \epsilon_{\mu_0}$, where n is the order of perturbation. These unavoidable divergences indicate that the Majorana composite polaritons consistently manifest as weak edge modes.

In order to test the locality of the Majorana polaritons, we evaluate the connected matrix element $\langle 0|\,\hat{c}_n\hat{a}\,|1\rangle_c = \langle 0|\,\hat{c}_n\hat{a}\,|1\rangle - \langle 0|\,\hat{a}\,|0\rangle\,\langle 0|\,\hat{c}_n\,|1\rangle$, given in perturbation theory by [59] [$n = (\sigma, j)$]

$$\langle 0|\,\hat{c}_n\hat{a}\,|1\rangle_c \simeq \psi_L^{1+}(n) + i\psi_R^{1+}(n). \qquad (11)$$

Other combinations of $\psi_\alpha^{1\pm}(n)$ ($\alpha = L/R$) are obtained from the connected matrix elements of $\hat{c}_n\hat{a}^\dagger$, $\hat{c}_n^\dagger\hat{a}$, and $\hat{c}_n^\dagger\hat{a}^\dagger$ between $|0\rangle$ and $|1\rangle$. They are calculated using the MPS wave functions and are illustrated in Figs. 5(a), 5(c).

Interestingly, these matrix elements all decay far from the edges and thus demonstrate both the resilient locality of the Majorana polaritons and their composite nature. We further quantify the photon mixing by introducing the weights of each component of the Majorana polaritons:

$$N_0^\alpha = \sum_n |\psi_\alpha^0|^2 N_1^\alpha = \sum_n |\psi_\alpha^{1+}|^2 + |\psi_\alpha^{1-}|^2, \qquad (12)$$

where $N_0^R = N_0^L$ and $N_1^R = N_1^L$ by symmetry. $\psi_\alpha^0(n)$ denotes the purely electronic components of the Majorana operators. These weights can also be calculated in perturbation theory. Numerically, we use Eq. (11) to define the weights, the results are shown in Figs. 5(b), 5(d). In order to quantify higher-order corrections, we compare the weight missing from the purely electronic component N_0, with the weight in the single photon component N_1. As expected at low enough values of g they perfectly match the perturbation theory prediction, while at higher couplings one would need to take into account higher-order corrections beyond Eq. (9). These are expected to involve multiphoton and multifermion operators which makes the Majorana-polariton expression more complicated; without breaking the quasiadiabatic arguments given in Sec. IV.

VI. CONCLUSIONS

We have shown that a one-dimensional topological superconductor with Majorana end modes is protected against the vacuum quantum fluctuations of an embedding cavity mode, despite its long-range nature. The quasiadiabatic approach explains this protection and reveals that Majorana evolves into Majorana polaritons to maintain topological order. We confirm this with DMRG simulations where topological markers are shown to persist through the cavity coupling, and the photonic component of Majorana polaritons is demonstrated up to strong cavity coupling. The main difference is that the Majorana polaritons are no longer assured to be strong edge modes. Instead, they can transition into weak edge modes where only the ground state is doubly degenerate. In the strong cavity coupling regime, mean-field techniques prove to be insufficient, making it crucial to account for light-matter entanglement. Our argumentation is highly general and is applicable to any 1D phase featuring end Majorana states, regardless of the nature of the cavity coupling, electric or magnetic. Even though not explicitly discussed, the results can be straightforwardly generalized to multimode cavities. The crucial prerequisite, however, is the absence of fermionic parity breaking induced by the cavity coupling.

Our results suggest that a qubit using Majorana polaritons also requires control over the cavity due to their hybrid nature [19]. We also anticipate that the topological insensitivity to vacuum cavity fluctuations will extend to other topological phases [66], in higher dimensions. For instance, in 2D class A models, such as the quantum Hall effect, the topology is robustly protected by a many-body Chern number [67]. This does not contradict recent works where finite-size effect and disorder [11,68] or coupling to external degrees of freedom [65] have been advocated to predict the loss of conductance quantization observed experimentally [18]. It would be interesting to build a comprehensive classification of cavity-embedded fermionic models in the spirit of recent classifications of interacting models [32,33].

ACKNOWLEDGMENTS

We acknowledge fruitful discussions with M. Dalmonte, C. Ciuti, T. Chanda, G. Chiriacò, O. Dmytruk, and M. Schirò. The DMRG numerical implementation is done via the ITensor library [69]. G.M.A. acknowledges funding from the European Research Council (ERC) under the European Union's Horizon 2020 Research and Innovation Program (Grant Agreement No. 101002955 – CONQUER).

---

[1] F. Schlawin, D. M. Kennes, and M. A. Sentef, Cavity quantum materials, Appl. Phys. Rev. **9**, 011312 (2022).
[2] J. Bloch, A. Cavalleri, V. Galitski, M. Hafezi, and A. Rubio, Strongly correlated electron–photon systems, Nature (London) **606**, 41 (2022).
[3] F. Mivehvar, F. Piazza, T. Donner, and H. Ritsch, Cavity QED with quantum gases: new paradigms in many-body physics, Adv. Phys. **70**, 1 (2021).
[4] F. J. Garcia-Vidal, C. Ciuti, and T. W. Ebbesen, Manipulating matter by strong coupling to vacuum fields, Science **373**, eabd0336 (2021).
[5] M. A. Sentef, M. Ruggenthaler, and A. Rubio, Cavity quantum-electrodynamical polaritonically enhanced electron-phonon coupling and its influence on superconductivity, Sci. Adv. **4**, eaau6969 (2018).
[6] J. B. Curtis, Z. M. Raines, A. A. Allocca, M. Hafezi, and V. M. Galitski, Cavity quantum Eliashberg enhancement of superconductivity, Phys. Rev. Lett. **122**, 167002 (2019).
[7] F. Schlawin, A. Cavalleri, and D. Jaksch, Cavity-mediated electron-photon superconductivity, Phys. Rev. Lett. **122**, 133602 (2019).
[8] S. Latini, D. Shin, S. A. Sato, C. Schäfer, U. D. Giovannini, H. Hübener, and A. Rubio, The ferroelectric photo ground state of $SrTiO_3$: Cavity materials engineering, Proc. Natl. Acad. Sci. USA **118**, e2105618118 (2021).
[9] Y. Ashida, A. İmamoğlu, J. Faist, D. Jaksch, A. Cavalleri, and E. Demler, Quantum electrodynamic control of matter: Cavity-enhanced ferroelectric phase transition, Phys. Rev. X **10**, 041027 (2020).
[10] K. Lenk, J. Li, P. Werner, and M. Eckstein, Dynamical mean-field study of a photon-mediated ferroelectric phase transition, Phys. Rev. B **106**, 245124 (2022).
[11] C. Ciuti, Cavity-mediated electron hopping in disordered quantum Hall systems, Phys. Rev. B **104**, 155307 (2021).
[12] A. Chiocchetta, D. Kiese, C. P. Zelle, F. Piazza, and S. Diehl, Cavity-induced quantum spin liquids, Nat. Commun. **12**, 5901 (2021).
[13] O. Dmytruk and M. Schirò, Controlling topological phases of matter with quantum light, Commun. Phys. **5**, 271 (2022).
[14] F. P. M. Méndez-Córdoba, J. J. Mendoza-Arenas, F. J. Gómez-Ruiz, F. J. Rodríguez, C. Tejedor, and L. Quiroga, Rényi entropy singularities as signatures of topological criticality in coupled photon-fermion systems, Phys. Rev. Res. **2**, 043264 (2020).
[15] L. Winter and O. Zilberberg, Fractional quantum Hall edge polaritons, arXiv:2308.12146.
[16] G. Jarc, S. Y. Mathengattil, A. Montanaro, F. Giusti, E. M. Rigoni, F. Fassioli, S. Winnerl, S. D. Zilio, D. Mihailovic, P. Prelovšek, M. Eckstein, and D. Fausti, Cavity-mediated thermal control of metal-to-insulator transition in 1T-TaS_2, Nature **622**, 487 (2023).
[17] G. L. Paravicini-Bagliani, F. Appugliese, E. Richter, F. Valmorra, J. Keller, M. Beck, N. Bartolo, C. Rössler, T. Ihn, K. Ensslin, C. Ciuti, G. Scalari, and J. Faist, Magneto-transport controlled by Landau polariton states, Nat. Phys. **15**, 186 (2019).
[18] F. Appugliese, J. Enkner, G. L. Paravicini-Bagliani, M. Beck, C. Reichl, W. Wegscheider, G. Scalari, C. Ciuti, and J. Faist, Breakdown of topological protection by cavity vacuum fields in the integer quantum Hall effect, Science **375**, 1030 (2022).
[19] D.-P. Nguyen, G. Arwas, Z. Lin, W. Yao, and C. Ciuti, Electron-photon Chern number in cavity-embedded 2D moiré materials, Phys. Rev. Lett. **131**, 176602 (2023).
[20] M. C. Dartiailh, T. Kontos, B. Douçot, and A. Cottet, Direct cavity detection of Majorana pairs, Phys. Rev. Lett. **118**, 126803 (2017).
[21] M. Trif and Y. Tserkovnyak, Resonantly tunable Majorana polariton in a microwave cavity, Phys. Rev. Lett. **109**, 257002 (2012).
[22] T. L. Schmidt, A. Nunnenkamp, and C. Bruder, Microwave-controlled coupling of Majorana bound states, New J. Phys. **15**, 025043 (2013).
[23] O. Dmytruk, M. Trif, and P. Simon, Cavity quantum electrodynamics with mesoscopic topological superconductors, Phys. Rev. B **92**, 245432 (2015).
[24] L. C. Contamin, M. R. Delbecq, B. Douçot, A. Cottet, and T. Kontos, Hybrid light-matter networks of Majorana zero modes, npj Quantum Inf. **7**, 171 (2021).
[25] O. Dmytruk and M. Trif, Microwave detection of gliding Majorana zero modes in nanowires, Phys. Rev. B **107**, 115418 (2023).
[26] G. M. Andolina, F. M. D. Pellegrino, V. Giovannetti, A. H. MacDonald, and M. Polini, Cavity quantum electrodynamics of strongly correlated electron systems: A no-go theorem for photon condensation, Phys. Rev. B **100**, 121109(R) (2019).
[27] K. Lenk, J. Li, P. Werner, and M. Eckstein, Collective theory for an interacting solid in a single-mode cavity, arXiv:2205.05559.
[28] P. Pilar, D. De Bernardis, and P. Rabl, Thermodynamics of ultrastrongly coupled light-matter systems, Quantum **4**, 335 (2020).
[29] A. Yu. Kitaev, Unpaired Majorana fermions in quantum wires, Phys. Usp. **44**, 131 (2001).
[30] C.-K. Chiu, J. C. Y. Teo, A. P. Schnyder, and S. Ryu, Classification of topological quantum matter with symmetries, Rev. Mod. Phys. **88**, 035005 (2016).
[31] H. Yao and S. Ryu, Interaction effect on topological classification of superconductors in two dimensions, Phys. Rev. B **88**, 064507 (2013).
[32] T. Morimoto, A. Furusaki, and C. Mudry, Breakdown of the topological classification $\mathbb{Z}$ for gapped phases of noninteracting fermions by quartic interactions, Phys. Rev. B **92**, 125104 (2015).
[33] L. Fidkowski and A. Kitaev, Effects of interactions on the topological classification of free fermion systems, Phys. Rev. B **81**, 134509 (2010).
[34] L. Fidkowski and A. Kitaev, Topological phases of fermions in one dimension, Phys. Rev. B **83**, 075103 (2011).

[35] A. Ghirri, C. Bonizzoni, M. Affronte, M. Maksutoglu, A. Mercurio, O. D. Stefano, S. Savasta, and M. Affronte, Ultrastrong magnon-photon coupling achieved by magnetic films in contact with superconducting resonators, Phys. Rev. Appl. **20**, 024039 (2023).

[36] J. Andberger, L. Graziotto, L. Sacchi, M. Beck, G. Scalari, and J. Faist, Terahertz chiral metamaterial cavities breaking time-reversal symmetry, arXiv:2308.03195.

[37] F. Tay, A. Mojibpour, S. Sanders, S. Liang, H. Xu, G. C. Gardner, A. Baydin, M. J. Manfra, A. Alabastri, D. Hagenmüller, and J. Kono, Ultrastrong photon-photon coupling, arXiv:2308.12427.

[38] A. Alexandradinata, N. Regnault, C. Fang, M. J. Gilbert, and B. A. Bernevig, Parafermionic phases with symmetry breaking and topological order, Phys. Rev. B **94**, 125103 (2016).

[39] F. Iemini, C. Mora, and L. Mazza, Topological phases of parafermions: A model with exactly solvable ground states, Phys. Rev. Lett. **118**, 170402 (2017).

[40] S. R. White, Density-matrix algorithms for quantum renormalization groups, Phys. Rev. B **48**, 10345 (1993).

[41] S. R. White, Density matrix formulation for quantum renormalization groups, Phys. Rev. Lett. **69**, 2863 (1992).

[42] U. Schollwöck, The density-matrix renormalization group in the age of matrix product states, Ann. Phys. (NY) **326**, 96 (2011).

[43] C.-M. Halati, A. Sheikhan, and C. Kollath, Theoretical methods to treat a single dissipative bosonic mode coupled globally to an interacting many-body system, Phys. Rev. Res. **2**, 043255 (2020).

[44] G. Passetti, C. J. Eckhardt, M. A. Sentef, and D. M. Kennes, Cavity light-matter entanglement through quantum fluctuations, Phys. Rev. Lett. **131**, 023601 (2023).

[45] Z. Bacciconi, G. M. Andolina, T. Chanda, G. Chiriacò, M. Schirò, and M. Dalmonte, First-order photon condensation in magnetic cavities: A two-leg ladder model, SciPost Phys. **15**, 113 (2023).

[46] A. M. Turner, F. Pollmann, and E. Berg, Topological phases of one-dimensional fermions: An entanglement point of view, Phys. Rev. B **83**, 075102 (2011).

[47] L. Fidkowski, Entanglement spectrum of topological insulators and superconductors, Phys. Rev. Lett. **104**, 130502 (2010).

[48] P. Fendley, Parafermionic edge zero modes in Z_n-invariant spin chains, J. Stat. Mech.: Theory Exp. (2012) P11020.

[49] A. S. Jermyn, R. S. K. Mong, J. Alicea, and P. Fendley, Stability of zero modes in parafermion chains, Phys. Rev. B **90**, 165106 (2014).

[50] J. Alicea and P. Fendley, Topological phases with parafermions: Theory and blueprints, Annu. Rev. Condens. Matter Phys. **7**, 119 (2016).

[51] Y. Oreg, G. Refael, and F. von Oppen, Helical liquids and Majorana bound states in quantum wires, Phys. Rev. Lett. **105**, 177002 (2010).

[52] R. M. Lutchyn, J. D. Sau, and S. Das Sarma, Majorana fermions and a topological phase transition in semiconductor-superconductor heterostructures, Phys. Rev. Lett. **105**, 077001 (2010).

[53] K. Flensberg, F. von Oppen, and A. Stern, Engineered platforms for topological superconductivity and Majorana zero modes, Nat. Rev. Mater. **6**, 944 (2021).

[54] S. Ryu, A. P. Schnyder, A. Furusaki, and A. W. W. Ludwig, Topological insulators and superconductors: tenfold way and dimensional hierarchy, New J. Phys. **12**, 065010 (2010).

[55] J. M. Luttinger, The effect of a magnetic field on electrons in a periodic potential, Phys. Rev. **84**, 814 (1951).

[56] J. Li, D. Golez, G. Mazza, A. J. Millis, A. Georges, and M. Eckstein, Electromagnetic coupling in tight-binding models for strongly correlated light and matter, Phys. Rev. B **101**, 205140 (2020).

[57] O. Dmytruk and M. Schiró, Gauge fixing for strongly correlated electrons coupled to quantum light, Phys. Rev. B **103**, 075131 (2021).

[58] A. Cottet, T. Kontos, and B. Douçot, Electron-photon coupling in mesoscopic quantum electrodynamics, Phys. Rev. B **91**, 205417 (2015).

[59] See Supplemental Material at http://link.aps.org/supplemental/10.1103/PhysRevB.109.165434 for a more detail discussion on the light-matter coupling, topology in absence of cavity, quasi-adiabatic continuation, perturbation theory, and numerical methods.

[60] G. M. Andolina, F. M. D. Pellegrino, A. Mercurio, O. D. Stefano, M. Polini, and S. Savasta, A non-perturbative no-go theorem for photon condensation in approximate models, Eur. Phys. J. Plus **137**, 1348 (2022).

[61] P. Nataf, T. Champel, G. Blatter, and D. M. Basko, Rashba cavity QED: A route towards the superradiant quantum phase transition, Phys. Rev. Lett. **123**, 207402 (2019).

[62] D. Guerci, P. Simon, and C. Mora, Superradiant phase transition in electronic systems and emergent topological phases, Phys. Rev. Lett. **125**, 257604 (2020).

[63] G. M. Andolina, F. M. D. Pellegrino, V. Giovannetti, A. H. MacDonald, and M. Polini, Theory of photon condensation in a spatially varying electromagnetic field, Phys. Rev. B **102**, 125137 (2020).

[64] S. S. Hegde and S. Vishveshwara, Majorana wave-function oscillations, fermion parity switches, and disorder in Kitaev chains, Phys. Rev. B **94**, 115166 (2016).

[65] V. Rokaj, J. Wang, J. Sous, M. Penz, M. Ruggenthaler, and A. Rubio, Weakened topological protection of the quantum Hall effect in a cavity, Phys. Rev. Lett. **131**, 196602 (2023).

[66] D. Shaffer, M. Claassen, A. Srivastava, and L. H. Santos, Entanglement and topology in Su-Schrieffer-Heeger cavity quantum electrodynamics, arXiv:2308.08588.

[67] Q. Niu, D. J. Thouless, and Y.-S. Wu, Quantized Hall conductance as a topological invariant, Phys. Rev. B **31**, 3372 (1985).

[68] G. Arwas and C. Ciuti, Quantum electron transport controlled by cavity vacuum fields, Phys. Rev. B **107**, 045425 (2023).

[69] M. Fishman, S. R. White, and E. M. Stoudenmire, The ITensor software library for tensor network calculations, SciPost Phys. Codebases, 4 (2022).